



Effects of poly (allylamine hydrochloride) as a new functionalization agent for preparation of poly vinyl alcohol/multiwalled carbon nanotubes membranes



Mohammad Amirilargani, Ali Ghadimi, Maryam Ahmadzadeh Tofighy, Toraj Mohammadi*

Research Centre for Membrane Separation Processes, Department of Chemical Engineering, Iran University of Science and Technology (IUST), Narmak, Tehran, Iran

ARTICLE INFO

Article history:

Received 29 May 2013

Received in revised form

20 July 2013

Accepted 22 July 2013

Available online 26 July 2013

Keywords:

Nanocomposite membrane

Multiwalled carbon nanotubes

Poly (vinyl alcohol)

Poly (allylamine hydrochloride)

Pervaporation dehydration

ABSTRACT

Using a solution technique, poly (allylamine hydrochloride)-wrapped multiwalled carbon nanotubes (MWNT-PAH) incorporated poly (vinyl alcohol) (PVA) membranes were prepared. Multiwalled carbon nanotubes (MWNTs) were synthesized via the CVD method using cyclohexanol and ferrocene as the carbon precursor and catalyst, respectively. The prepared membranes were characterized by Fourier transform infrared spectroscopy (FTIR), field emission scanning electron microscopy (FESEM) and atomic force microscopy (AFM). The prepared membranes were subjected to pervaporation (PV) dehydration of isopropanol (IPA). MWNTs wrapped with PAH were well dispersed in the polymer matrix in comparison with prepared MWNTs. Degree of swelling (DS) of the prepared membranes decreased by addition of MWNT-PAH into the PVA matrix. Furthermore, PV results revealed that incorporation of modified carbon nanotubes (CNTs) into the PVA matrix increases water selectivity significantly due to rigidification of the polymer chains. The nanocomposite membrane containing 1 wt% of MWNT-PAH exhibited excellent PV properties. Permeation flux and separation factor were $.229 \text{ kg/m}^2 \text{ h}$ and 141.2 for the raw PVA and $.207 \text{ kg/m}^2 \text{ h}$ and 948.4 for the membrane prepared with 1 wt% of MWNT-PAH respectively. Separation factor decreased significantly by further addition of MWNT-PAH due to its agglomeration in the PVA matrix.

© 2013 Elsevier B.V. All rights reserved.

1. Introduction

Pervaporation is a membrane separation technology with high selectivity, efficiency and energy saving benefits, especially in separating close-boiling and azeotropic mixtures [1,2]. In recent years, pervaporation membranes have been developed for various applications such as dehydration of organic solvents, purifying aqueous streams by removal of dilute organic compounds and separation of organic–organic mixtures [3]. In the literature, PVA has been widely used in PV dehydration of organics [4] due to its outstanding membrane forming ability, easy processing and abundant availability, but its excessive swelling in aqueous media tends to lower its water selectivity. Blending, crosslinking, and incorporating with inorganic fillers are mostly used methods to reduce membrane swelling [5,6], though a trade-off relationship between membrane permeability and selectivity is often observed. So, recent research efforts have been focused on developing new types of membranes, where nanofillers are dispersed in a polymer

matrix, and such membranes are sometimes known as nanocomposite membranes [7,8]. Organic–inorganic hybrid membranes could be prepared by simply embedding inorganic particles such as zeolites, silica, carbon molecular sieves and activated carbons [9–11]. Recently carbon nanotubes (CNTs) have also attracted significant attention as a new type of nanofillers for fabrication of novel polymeric nanocomposite membranes [12]. Strong interfacial interaction between CNTs and polymer matrix is required for good dispersion of CNTs [13]. However, this condition is extremely difficult to achieve with raw CNTs, which are well known for their chemical inertness and strong tendency to agglomerate into stabilized bundles due to the strong van der Waals forces. Homogeneous dispersion within polymer matrix and improved CNTs/matrix wetting and adhesion are effective factors in preparation of polymer/CNTs nanocomposites. So, functionalization of CNTs with specific functional moieties is necessary to reduce the van der Waals forces and enable CNTs to interact with hydrophilic polymer [14]. Surface oxidation and attachment of hydrophilic functional groups onto the CNT surface, chemical functionalization and attachment of polar groups to the CNT sidewall, surface coating by non-covalent interaction with a third phase dispersant such as polymers, surfactants and DNA are the methods which have been

* Corresponding author. Tel.: +98 21 77240496; fax: +98 21 77240495.
E-mail address: torajmohammadi@iust.ac.ir (T. Mohammadi).

widely used for homogeneous dispersion of CNTs in polymer matrixes [15–22]. Each of these strategies has its own advantages and disadvantages. Covalent sidewall functionalization can improve dispersion of CNTs but may destroy the perfect atomic structures of CNTs and degrade its mechanical properties [23]. In comparison with covalent methods, intrinsic properties and graphitic structure of CNTs may be maintained under mild reaction conditions of non-covalent functionalization but their dispersion is not very stable [22,24]. Non-covalent methods with deposition of polyelectrolyte, macromolecules or even nanoparticles on the surface of multiwalled carbon nanotubes (MWNTs) are preferred over covalent surface modification as they do not require acid treatment [25–27]. Among polymers selected for modification of CNTs, water soluble polymers are very attractive because functions of both polymers and CNTs can be tailored to create one object [28]. Peng et al. [29] used β -cyclodextrin as the functionalization agent to improve dispersion of CNTs in PVA solution. They used these membranes for PV separation of benzene/cyclohexane mixtures, and showed excellent PV performances. Also, Sajjan et al. [30] investigated effects of CNTs content wrapped with chitosan on pervaporation performance of sodium alginate membranes. Their results showed that addition of CNTs modified with chitosan enhances both permeation flux and separation factor for dehydration of isopropanol (IPA). Spinks et al. [31] showed that dispersion of CNTs in polymer matrix can affect mechanical properties of chitosan/CNTs. They improved dispersion of CNTs by sonic agitation, and then centrifugation to remove their aggregates.

Poly (allylamine hydrochloride) (PAH) is a cationic polyelectrolyte which has been used for wrapping the CNTs. It was investigated that MWNTs wrapped with PAH are stable for a long time in an aqueous solution [32]. To our knowledge, there is no information about effects of PAH as a functionalization agent for preparation of PVA nanocomposite membranes. In this research, PAH was used as a noncovalent functionalization agent for better dispersion of MWNTs. The functionalized MWNTs were incorporated into PVA solutions to prepare PVA/MWNT–PAH nanocomposite membranes for pervaporation dehydration of IPA.

2. Experimental

2.1. Materials

PVA (MW: 130,000) with a degree of hydrolysis of more than 98%, PAH (MW = 58,000), glutaraldehyde (GA, 25 wt% in H₂O) and hydrochloric acid were all purchased from Sigma-Aldrich. Polyacrylonitrile (PAN, MW = 150,000) supplied by Sigma-Aldrich was used as polymer for preparation of the ultrafiltration (UF) membrane support. N-methyl-2-pyrrolidone (NMP) was used as solvent from Sigma-Aldrich. Polyvinylpyrrolidone (PVP K15, MW = 15,000) supplied by Fluka was used as a pore former hydrophilic additive. Ferrocene as catalyst (purity $\geq 98\%$, B.D.H.) and cyclohexanol (purity $\geq 98\%$, Fluka) as carbon precursor were used to synthesize the CNTs.

2.2. Support (UF membrane) preparation

PAN polymer flakes absorb moisture very rapidly. Therefore, these flakes were dried for more than 12 h at 80 °C prior to preparation of the casting of solution. Deionized water was used as the main non-solvent in coagulation bath. At first, for preparation of the PAN porous support membrane, a solution of 16 wt% PAN and 2 wt% PVP in NMP was prepared [33,34]. Then, the solution was mixed by stirring for 8 h at a temperature of 50 °C. The stirring was carried out at 150 rpm. When necessary, an ultrasonic

bath (BANDELIN, Sonorex Digitec, GERMANY) was employed to remove any air bubbles from the polymeric casting solution. After that the prepared homogeneous solution was cast using a film applicator to 150 μm clearance gap on a polyester (PET) nonwoven fabric. The cast film was subsequently immersed in a distilled water bath for 24 h to complete the phase separation, where exchange between the solvent (NMP) and the non-solvent (water) was induced. This was performed to ensure the complete removal or evaporation of residual solvent from the membranes.

2.3. Synthesis of MWNTs

The MWNTs were synthesized via chemical vapor deposition (CVD) of a gas mixture evaporated from the catalyst powder and the liquid carbon source. The CVD system consisted of a horizontal stainless steel reactor (.700 m long, .032 m in diameter) housed in a one stage cylindrical furnace. A flask (steel container) containing reagents was connected to the reactor. The reagents were prepared by dissolving ferrocene (purity $\geq 98\%$, B.D.H.) in cyclohexanol with a mass ratio of 1:20. Evaporation of the reagents was performed using an oil bath. Nitrogen was used as a carrier gas and fed to the reactor close to the reagent inlet to carry the gas mixture of precursors towards the center of the furnace, where pyrolysis of the gases took place. Cyclohexanol as the carbon source was selected due to its hexagonal carbon ring structure and its low boiling point (160 °C) [35–37]. Furthermore, it is a good solvent for ferrocene and this allows constitution of a homogeneous solution. Ferrocene was used as the catalyst, since it is a good precursor for production of iron nanoparticles, which play the role of catalyst in the formation of MWNTs [38,39]. The MWNTs were characterized before and after purification.

2.4. MWNT modification with PAH

MWNTs were dispersed in the PAH salty solution (.5 M NaCl, 500 ml) and the mixture was sonicated for 4 h, stirred overnight at 80 °C, and again sonicated for 3 h. The excess PAH was removed with water and by centrifugation until a stable, homogeneous MWNT/PAH suspension was obtained [32]. PAH confers to MWNTs amine functionality and this ensures good stability due to electrostatic interactions in water and organic solvents.

2.5. Membrane preparation

The PVA/MWNTs–PAH nanocomposite membranes were prepared via solution casting and solvent evaporation technique. PVA was dissolved in deionized water at 90 °C and then the solution was stirred for a period of time to make it homogeneous. The solution was filtered through a glass fiber filter to remove insoluble impurities and then vacuumed to remove any bubbles. Simultaneously the modified MWNTs/PAH were dispersed in deionized water, and then exposed to ultrasonication for 2 h. These two solutions were mixed and stirred for 12 h. In situ crosslinking was performed by adding GA and hydrochloric acid to the resulting solution and further stirring. The resulting solution was cast on the synthesized PAN UF membrane which was cast on a PET nonwoven fabric. The nanocomposite membrane was dried at room temperature and then annealed at 90 °C. The procedure of membrane preparation is shown in Fig. 1. The mass ratio of MWNT–PAH to PVA was varied at 0%, .5%, 1%, 2%, 3% and 4%.

2.6. Membrane characterization

2.6.1. Infrared absorbance characteristics

The chemical structure changes of nanocomposite membranes with different contents of MWNT–PAH were monitored by a Fourier

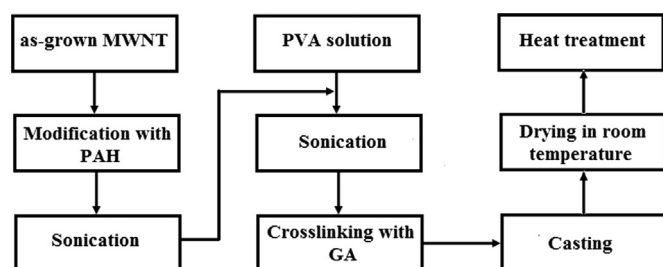


Fig. 1. Preparation procedure of the PVA/MWNT-PAH nanocomposite membranes.

transform infrared (FTIR) spectrum. The FTIR spectra were obtained using a VERTEX spectrometer (VERTEX 80, BRUKER, GERMANY) equipped with an attenuated total reflectance (ATR) accessory. The scanning range was 650–4000 cm^{-1} . The experiment was performed in air atmosphere at ambient temperature.

2.6.2. Field emission scanning electron microscope (FESEM)

A field emission scanning electron microscope (FESEM) (MIRA 3 LM, TESCAN Inc., USA) was used for analysis of the PVA/PAH-MWNTs nanocomposite membranes. The membranes were cut into small pieces. The dried samples were gold sputtered to be electrically conductive. The micrographs were taken in high vacuum conditions at 5 kV.

2.6.3. High resolution transmission electron microscopy (HR-TEM)

Morphology of the as prepared MWNT and the PAH-wrapped MWNT samples were studied using a HR-TEM (PHILIPS, CM30) operating at 200 kV. MWCNTs were prepared for TEM observations by dispersing them in acetone with the aid of an ultrasonicator. The HR-TEM samples were obtained by putting a drop of the solutions onto standard holey carbon grids, and letting the solvent evaporate.

2.6.4. Atomic force microscopy (AFM)

AFM analysis was applied to evaluate roughness and surface morphology of the prepared membranes using a DualScope™ scanning probe-optical microscope (DME model C-21, Denmark). Membrane samples (approximately 1 cm^2) were fixed on the specimen holder and 5 × 5 μm areas were scanned in the tapping mode in air. The surface roughness parameters are reflected in terms of the average roughness (S_a), the root mean square of the Z data (S_q) and the mean difference between the highest peaks and the lowest valleys (S_z).

2.7. PV experiment

The prepared membranes were evaluated in a PV separation system. Mixtures of IPA–water were prepared and held in a feed tank with a volume capacity of 1 L. Effective surface area of the membranes in the PV cell was .00158 m^2 . PV apparatus was made of a stainless steel cell in which the feed stock solution was maintained at the required constant temperature controlled thermostatically with a water jacket. The PV cell consisted of an efficient three-blade stirrer powered by a DC motor in the feed compartment. The permeate pressure was maintained at 5 mm Hg using a vacuum pump (Platinum JB, USA). Before starting the PV experiment, the test membrane was equilibrated for 1 h with the feed mixture and after establishment of the steady state equilibrium, the liquid permeate was collected and condensed in traps under liquid nitrogen atmosphere. Concentrations of the feed and the permeate were measured using an Abbe refractometer (NAR-3T ATAGO, Japan) by comparing the observations with a standard graph of refractive index versus

feed mixture composition (calibration curve). Permeation properties of the membranes were characterized by separation factor (S.F.), total permeation flux (J) and PV separation index (PSI) using the following equations, respectively:

$$J = \frac{W}{A \times t} \quad (1)$$

$$\text{S.F.} = \frac{Y_W/Y_{\text{IPA}}}{X_W/X_{\text{IPA}}} \quad (2)$$

$$\text{PSI} = J(\text{S.F.} - 1) \quad (3)$$

where W is the mass of permeate (kg); A is the effective membrane area (m^2); t is the permeation time (h); and Y_W and Y_{IPA} are the mass percent of water and IPA in the permeate, respectively. X_W and X_{IPA} are the respective mass percent of water and IPA in the feed.

2.7.1. Swelling study

Swelling experiments on the membranes were performed gravimetrically at 30 °C in 10 wt% water containing feed mixtures. This experiment is helpful to investigate the interactions of the membranes with the liquid penetrants. The membranes were dried completely at 70 °C for 6 h and weighed by a digital microbalance (SARTORIUS AG GERMANY) sensitive to $\pm .01$ mg. These membranes were immersed in the water–IPA mixtures in a sealed vessel at 30 °C for 48 h to allow them to reach their equilibrium swelling. The swollen membranes were weighed as quickly as possible after being wiped with tissue papers. Each run was performed at least three times, and the results were averaged. The percentage degree of swelling (DS %) was calculated as

$$\text{Degree of swelling (DS) (\%)} = \left(\frac{W_s - W_d}{W_d} \right) \times 100 \quad (4)$$

where W_s and W_d are the weights of the swollen and the dried membranes, respectively.

3. Results and discussion

3.1. Characterization of MWNTs

FESEM and TEM images of the as-grown MWNTs by the CVD method are illustrated in Fig. 2. As observed, the prepared MWNTs have appropriate density and are entangled. Obviously, as it can be observed, the synthesized MWNTs are free of amorphous carbon and also deactivated metallic particles are significantly low. This can be attributed to the presence of oxygen atoms in cyclohexanol [40]. Oxygen atoms in cyclohexanol can oxidize amorphous carbon and consequently the synthesized MWNTs are free of amorphous carbon. This conclusion is consistent with the results of experiments in which adding 2 mol% of acetic acid to xylene as the carbon precursor declined amorphous carbon [41]. Generally, deposition of amorphous carbon on the catalyst surface increases formation of amorphous carbon. However, using cyclohexanol as the carbon precursor reduces formation of amorphous carbon. The presence of oxygen atoms in cyclohexanol causes in situ oxidation of amorphous carbon [40]. This reduction of amorphous carbon prevents the catalyst surface from being passive. HR-TEM image of a MWNT (Fig. 2b) confirms that the MWNTs are multiwalled and also have highly pure structure [42]. Polymer wrapping is one of the most common methods for functionalization of MWNTs [32]. TEM image of the PAH-wrapped MWNTs is presented in Fig. 3. As observed, PAH covers completely the surface of MWNTs. With intrinsic van der Waals forces, MWNTs are typically held together as bundles in most solvents. The PAH chains are non-covalently adsorbed around the CNTs due to van der Waals interactions,

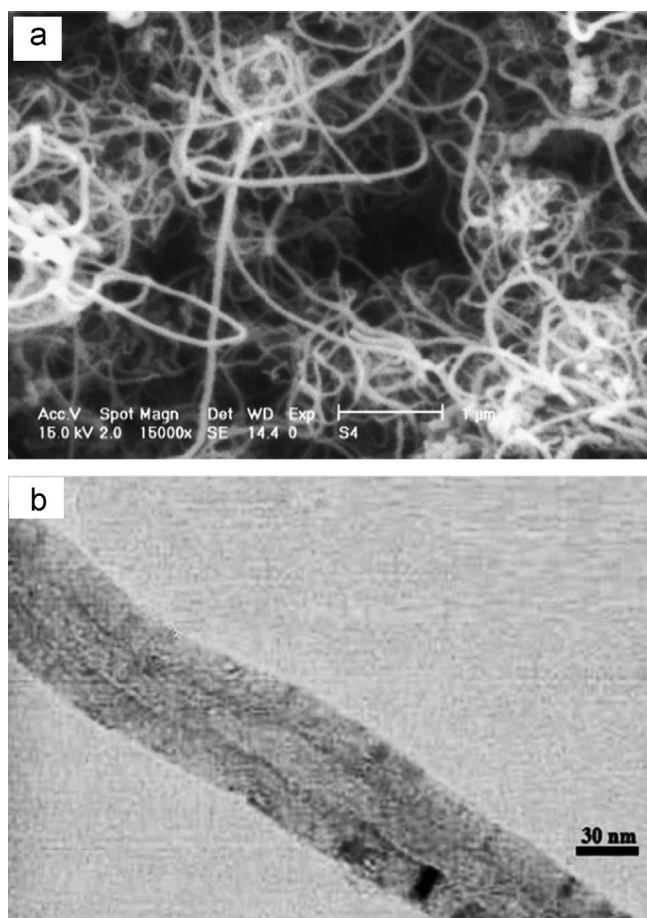


Fig. 2. (a) FESEM and (b) HR-TEM images of the as-grown MWNTs.

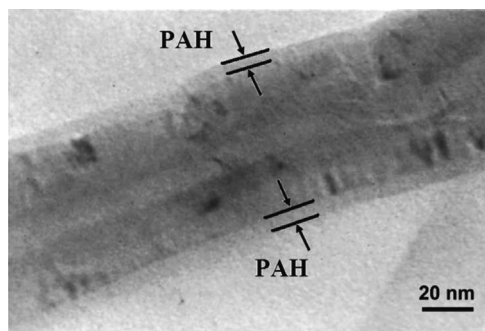


Fig. 3. HR-TEM image of the PAH-wrapped MWNTs.

mechanical wrapping and anchoring. The charged amine functionalities on the MWNTs surface ensure good stability due to the electrostatic interactions (repulsions) in aqueous solutions [43]. As the pristine structures of the MWNTs are not changed, the unique properties of the pristine MWNTs have been compromised. By combining the properties of MWNTs and the versatility and biocompatibility of PAH, these PAH functionalized MWNTs can find potential applications in different fields.

3.2. FTIR results of PVA nanocomposite membranes

ATR-IR spectra of the nanocomposite membranes in the range of 500–4000 cm^{-1} are presented in Fig. 4. The FTIR spectra of raw PVA membrane show characteristic broad absorbances at 1087 cm^{-1} (C–O groups), at 1245 cm^{-1} (C–O–C groups), at 2931 cm^{-1} (symmetric $-\text{CH}_2-$) and at 3200–3400 cm^{-1} for $-\text{OH}$ stretching. In the

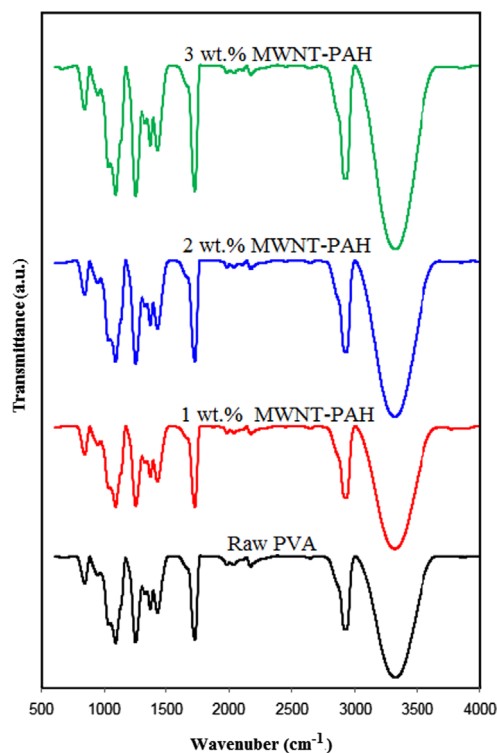


Fig. 4. ATR-FTIR spectra of PVA membranes with different MWNT-PAH loadings.

nanocomposite membranes, no further absorption peak is observed [44]. This can be attributed to the fact that the functional groups of the nanocomposite PVA/MWNT-PAH membranes are the same as those of the raw PVA membrane.

3.3. FESEM images of PVA nanocomposite membranes

The PVA solution was cast on the PAN UF membrane layer which was prepared on the PET nonwoven fabric. FESEM images of the nanocomposite membranes are illustrated in Fig. 5. The PAN support has suitable porosity and provides good mechanical strength for the PVA selective layer. As shown in Fig. 5b, thickness of the PVA layer cast on the PAN support is around 15 μm . Dispersed inorganic phase and continuous organic phase affect the nanocomposite membranes separation properties and morphology. Surface FESEM images of the nanocomposite membranes are presented in Fig. 6. Obviously, the raw PVA membrane is free of MWNTs particles and by increasing MWNTs loading the number of light dots which present the MWNT's tips increases. Surface FESEM images also indicate that MWNT-PAH particles are not agglomerated and well distributed along the surface of PVA matrix with only a few areas of agglomeration in lower concentration of MWNT-PAH. In Fig. 6d and e dotted circles exhibit the agglomerated MWNTs. As observed in Fig. 6(a–c), the number of MWNTs particles increases by increasing the MWNT-PAH content from 0 to 1 and 2 wt%. Also, there is no obvious agglomerated MWNT-PAH compared with Fig. 6(d, e). Also, the number of these particles decreases in the surface of the prepared membranes with 3 and 4 wt% of MWNT-PAH and there are some agglomerated MWNT-PAH particles in their surface structure. Each agglomerated MWNT-PAH is formed from a large number of MWNT-PAH particles. In the surface structure of the membrane prepared from 4 wt% of MWNT-PAH due to the high concentration of MWNTs, there are both agglomerated MWNT-PAH and MWNT-PAH particles.

The good adhesion between the PAH modified MWNTs and the PVA is due to the high compatibility between the MWNTs and the

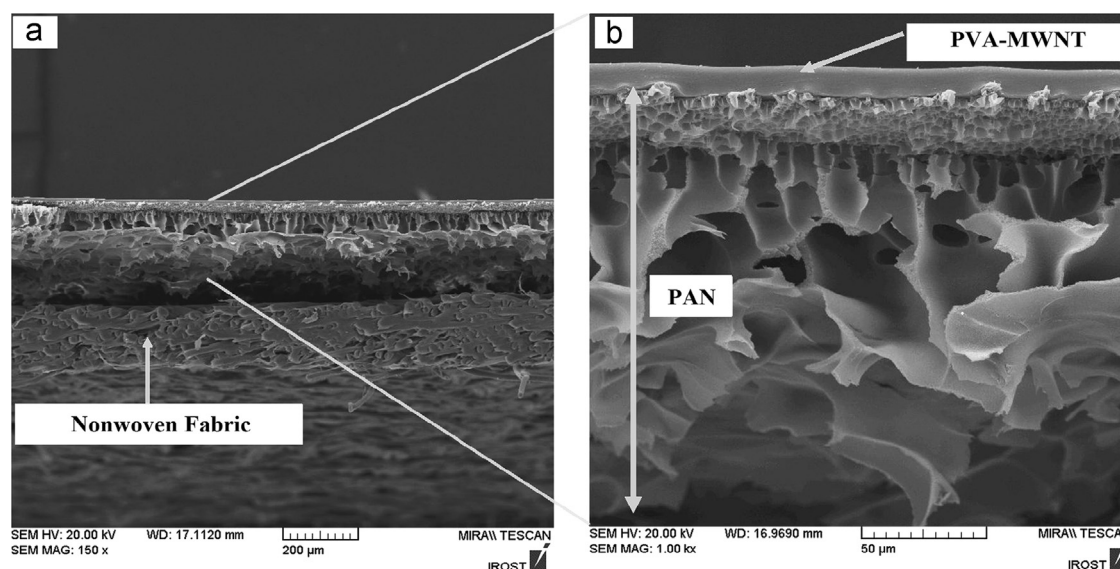


Fig. 5. PVA nanocomposite membrane on the PAN support layer.

hydrophilic PVA matrix. Cross sectional FESEM images of the prepared PVA nanocomposite membranes with different loadings of MWNT–PAH are illustrated in Fig. 7. Cross sectional FESEM images of the membranes prepared with 1 and 2 wt% of MWNT–PAH also reveal that MWCNTs particles are well distributed throughout the PVA matrix. There is also no evidence of interface voids or sieve in cage morphology of these membranes. This affinity between the PVA matrix and the MWCNTs particles is due to the PAH which was used for wrapping MWCNTs. As observed in FESEM cross sectional images, modification of MWCNTs with PAH increases the affinity of MWCNTs to PVA. By increasing the MWNT–PAH concentration to 3 and 4 wt%, the agglomeration of MWCNTs nanoparticles occurs in the cross section of PVA matrix.

3.4. AFM images of PVA nanocomposite membranes

Two and three dimensional surface AFM images of the PAH–MWNT/PVA nanocomposite membranes prepared with different contents of PAH–MWNT are presented in Fig. 8. In these images, the brightest area represents the highest point of the membrane surface and the dark regions indicate the valleys. As observed, the neat PVA membrane prepared with no PAH–MWNT obviously exhibits smoother surface with no roughness. Surface roughness parameters of the membranes explained in terms of the mean roughness (S_a), the root mean square of the Z data (S_q), and the mean difference between the highest peaks and the lowest valleys (S_z) were calculated by SPM DME software. In this study, several AFM images were taken for each membrane. The surface roughness values were almost similar in different AFM surface images taken for each membrane. The averaged results obtained are presented in Table 1. As observed, the roughness parameters of the PVA nanocomposite membranes increase with the PAH–MWNT content. The mean roughness (S_a) of the neat PVA membrane severely increases from 6.19 to 32.42, 62.47 and 271.14 nm by addition of 1, 2 and 3 wt% of PAH–MWNT to the neat PVA membrane. In low concentrations of functionalized CNTs, because of less electrostatic interactions among the MWCNTs, they are regularly collocated in the membrane and the membrane surface becomes smoother [45]. However, as observed in the surface FESEM images (Fig. 6), due to the agglomeration of CNTs, roughness of the membrane surface increases by increasing the MWCNTs concentration.

3.5. Effect of MWNT–PAH content on membrane swelling

In PV, membrane swelling plays a key role and controls transport of permeating molecules under the influence of chemical potential gradient. The swelling behavior of the prepared membranes is illustrated in Fig. 9. As observed, the raw PVA membrane shows higher DS compared with the nanocomposite PVA membranes prepared with different contents of the MWNT–PAH. Obviously, increasing MWNT–PAH content in PVA matrix is responsible for the reduction of swelling. This can be attributed to the fact that the CNTs increase the extent of rigidification [46]. Rigidification consequently decreases mobility and free volume of the polymer chains. Moreover, the surface hydrophilicity of PVA nanocomposite membranes decreases by increasing the MWNT–PAH content in PVA matrix [47]. PVA in its crystal state is more difficult to be dissolved in water than in its amorphous state because of stronger intermolecular hydrogen bonds among PVA molecules in the crystal state [46–48]. However, DS increases as the content of MWNT–PAH increases from 1 to 2, 3 and 4 wt% in the casting PVA solution. Obviously, changing the membrane structure and increasing the free-volume are two factors which are responsible for the enhanced DS with increase in the MWNT–PAH content in PVA membrane matrix. Aggregation of the MWCNTs decreases the compactness of PVA membrane and penetrants can permeate through the membrane more readily. Also, reduction of polymer chain packing may increase free volume of the polymeric membrane [46]. Finally, it can be concluded that there is an optimum MWNT–PAH content at which the extent of rigidification is more dominant. At higher MWNT–PAH content, the extent of aggregation is more dominant.

3.6. PV performance

3.6.1. Effect of MWNT–PAH on PV performance

The effect of MWNT–PAH content on the PV performance of the nanocomposite membranes is shown in Fig. 10. Operating conditions were fixed at 10 wt% water in IPA mixture and feed temperature of 30 °C. As shown, selectivity of the prepared membranes increases with the MWNT–PAH content in the casting solution compared with the membrane prepared with no MWNT–PAH. Generally, by increasing density of membrane either by increasing packing density or by incorporating another polymer or filler in the membrane matrix, permeation flux decreases and

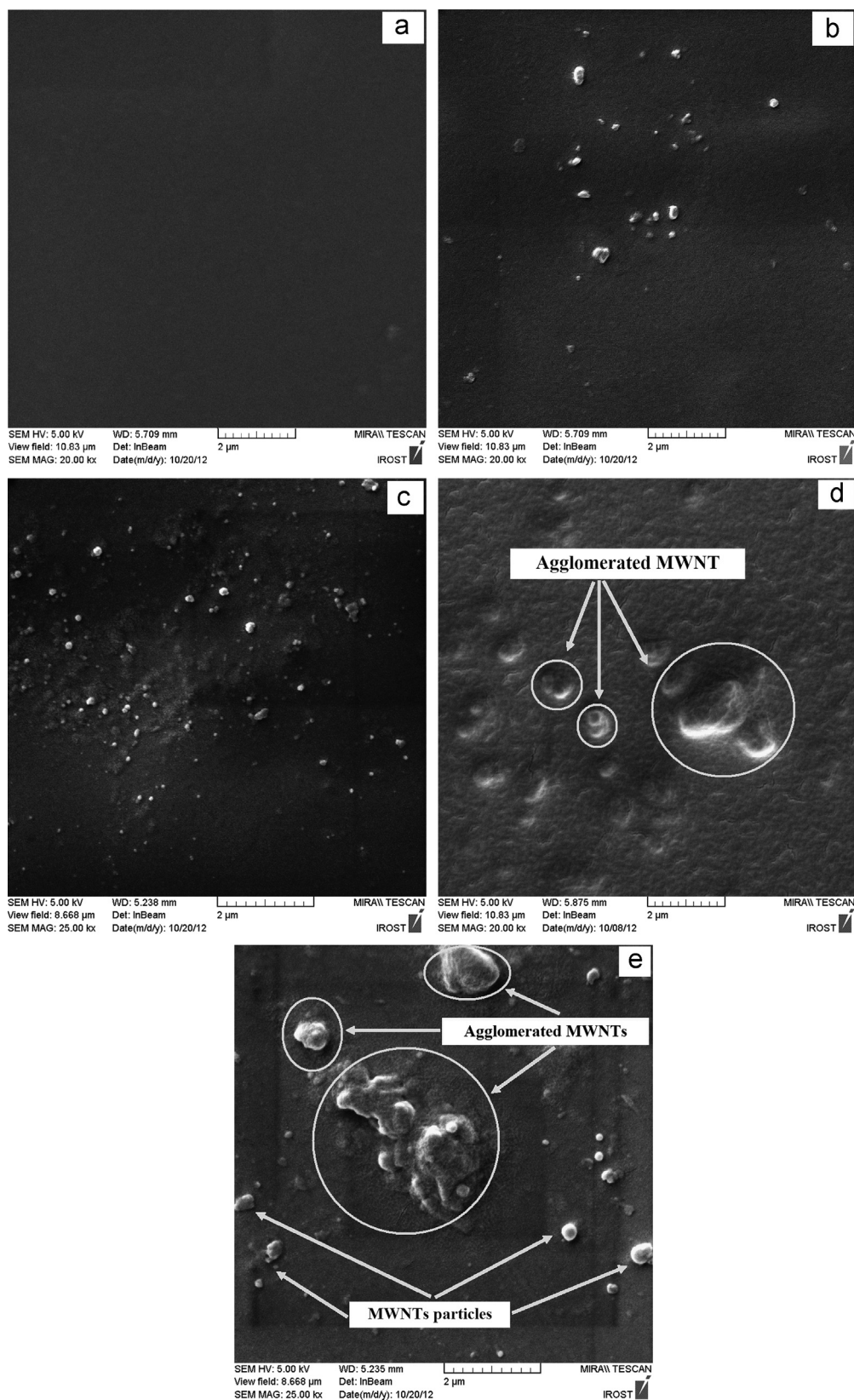


Fig. 6. Surface FESEM images of PVA nanocomposite membranes prepared with different contents of MWNT-PAH: (a) raw PVA, (b) 1 wt%, (c) 2 wt%, (d) 3 wt% and (e) 4 wt%.

selectivity increases [49]. This can be attributed to the fact that the MWNT-PAH in the PVA matrix acts as reinforcing bridge elements and makes PVA chains more rigid, thereby giving a reduced DS with a simultaneous permeation flux reduction. The PVA

membrane prepared with no MWNT-PAH with higher DS shows the highest permeation flux compared with other nanocomposite membranes. Also, permeation flux of the nanocomposite membranes follows their DS behavior. Incorporation of the MWNT-PAH

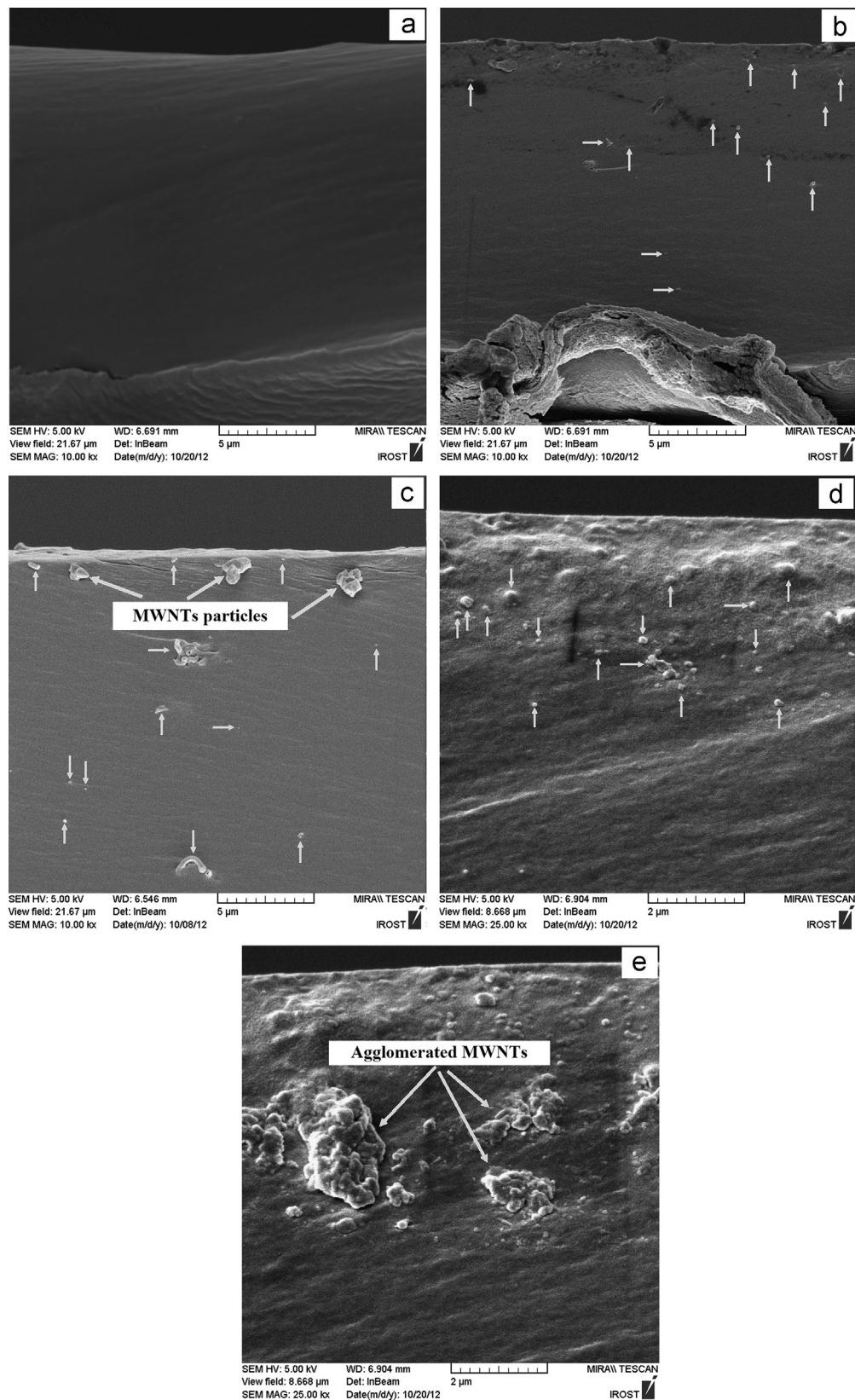


Fig. 7. Cross sectional FESEM images of PVA nanocomposite membranes with different contents of MWNT-PAH: (a) raw PVA, (b) 1 wt%, (c) 2 wt%, (d) 3 wt% and (e) 4 wt%.

into the PVA matrix has two main effects on permeation flux of the nanocomposite membranes. Firstly, permeation flux increases due to the nanochannels of MWNT-PAH [50]. Secondly, loading of the MWNT-PAH reduces the membrane free volume and this will

reduce permeability. As observed in Fig. 10, addition of .5 and 1 wt % of the MWNT-PAH to the PVA matrix decreases permeation flux. For example, permeation flux decreases from .229 to .209 $\text{kg}/\text{m}^2 \text{ h}$ by increasing the MWNT-PAH loading from 0 to 1 wt% and then

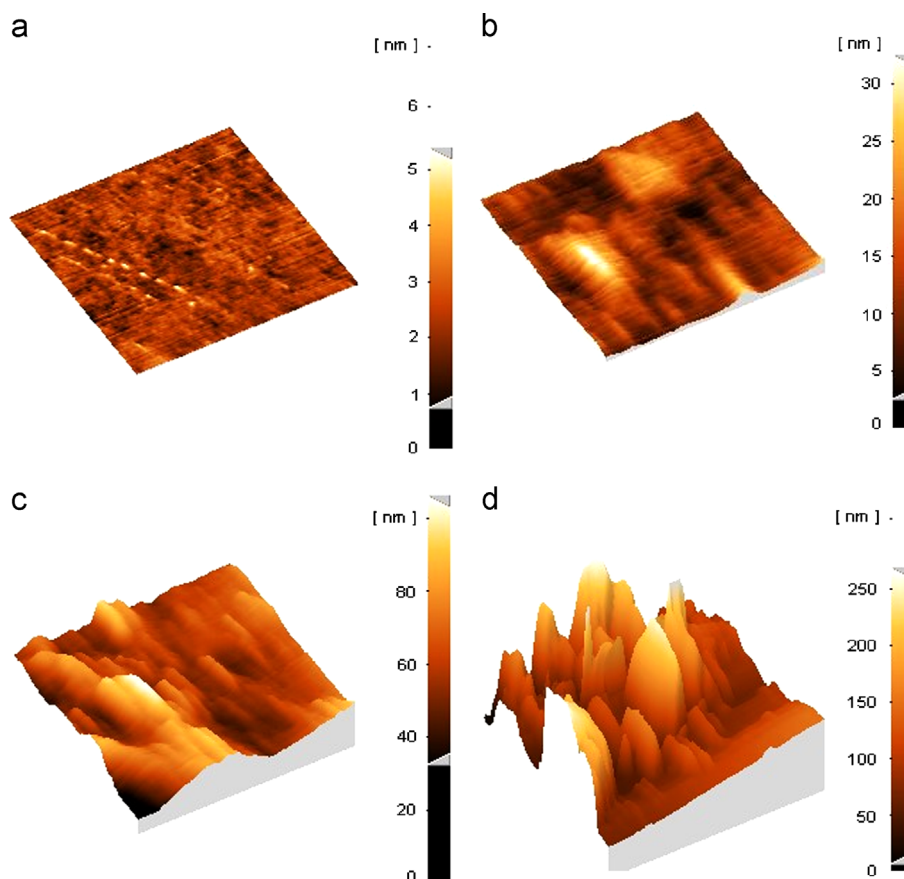


Fig. 8. Three dimensional AFM surface images of PVA nanocomposite membranes prepared with different contents of MWNT-PAH: (a) raw PVA, (b) 1 wt%, (c) 2 wt% and (d) 3 wt%.

Table 1

Surface roughness parameters of the PVA/MWNT-PAH membranes obtained from the AFM images.

Membrane	Roughness parameters		
	S_a (nm)	S_q (nm)	S_z (nm)
Raw PVA	6.19	.42	.55
1 wt% MWNT-PAH	32.42	3.67	4.81
2 wt% MWNT-PAH	62.47	9.71	12.60
3 wt% MWNT-PAH	271.14	34.23	46.14

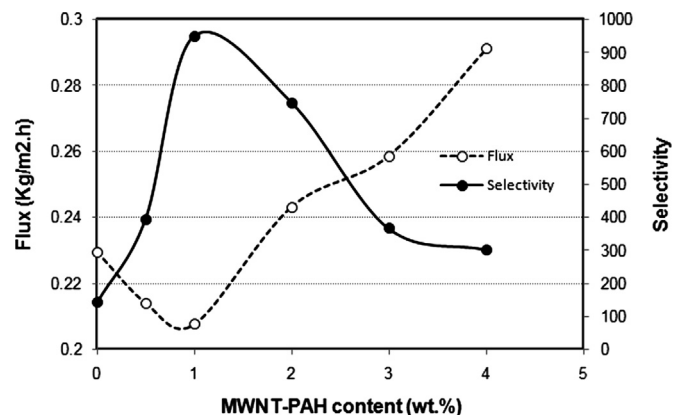


Fig. 10. Effect of MWNT-PAH loading on PV performance of different PVA nanocomposite membranes using 10 wt% water in IPA mixture at 30 °C.

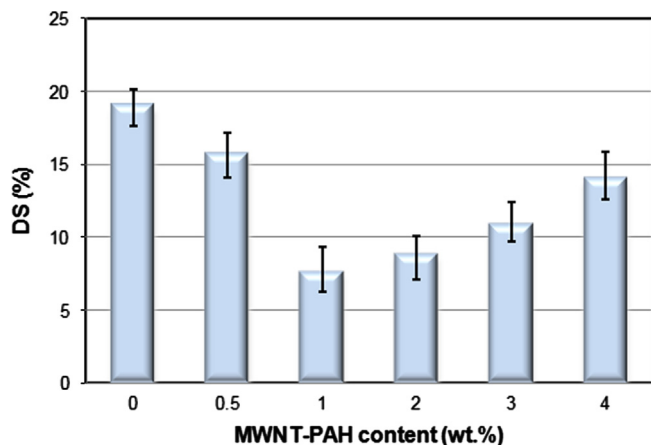


Fig. 9. Effect of MWNT-PAH loading on DS of PVA nanocomposite membranes.

increases by further addition of the MWNT-PAH. Free volume reduction of the nanocomposite membranes prepared with the MWNT-PAH may reduce permeation flux. As shown in the FESEM images, the agglomeration of MWNT-PAH increases at higher MWNT-PAH contents. The agglomerated MWNT-PAH increases the membrane free volume and consequently penetrants can permeate through the membranes more readily. Also, the higher DS of prepared membranes at higher content of MWNT-PAH confirms the permeation behavior of the membranes. On the other hand, selectivity of the prepared membranes increases from 141.2 to 948.4 by increasing the MWNT-PAH content from 0 to

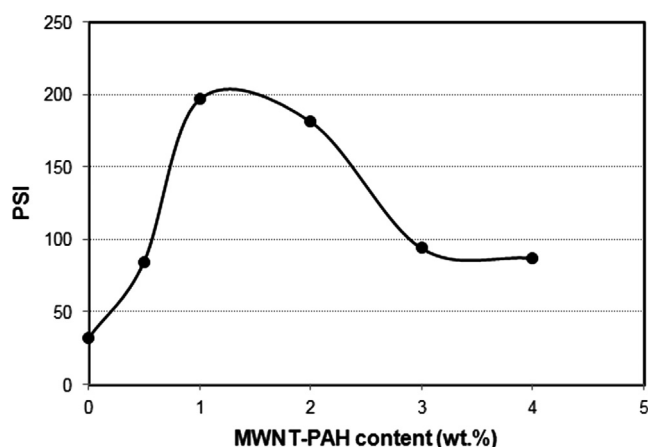


Fig. 11. Effects of MWNT-PAH loading on PSI of different PVA nanocomposite membranes.

Table 2

Comparative study of PV performance of the prepared nanocomposite membranes with the membranes reported in the literature for dehydration of IPA (operating condition: 10 wt% water at 30 °C).

Membrane	Flux (kg/m ² h)	Selectivity	PSI	Ref.
PVA/(APTEOS+TEOS)	.06	891	53.4	[51]
PVA/APTEOS	.0265	1580	41.84	[52]
PVA/Fe	.084	144	12.01	[53]
PVA/silicalite	.084	1295	108.67	[54]
PVA/KA	.179	410	73.21	[55]
PVA/NaA	.183	328	59.84	
PVA/CaA	.193	233	44.77	
PVA/NaX	.216	233	50.11	
PVA/oxidized MWNT	.079	1794	141.32	[46]
PVA/MWNT-PAH (1 wt%)	.207	948.4	196.68	This work

1 wt%. In order to investigate the overall performance of membranes, pervaporation separation index (PSI) for all the membranes at 30 °C using a mixture of 10 wt% water in IPA was calculated as presented in Fig. 11. As observed, PSI values increase with increase in the MWNT-PAH content up to 1 wt% and then decrease by further increasing to 2, 3 and 4 wt%. The reduction of PSI values for the nanocomposite membranes prepared at the higher content of MWNT-PAH can be due to the sharp reduction of selectivity. As observed, the nanocomposite membrane prepared with 1 wt% of MWNT-PAH exhibits the highest PSI value compared with the other membranes.

3.6.2. Comparison of the nanocomposite membranes with the literature

The obtained results in the present work were compared with the literature. Table 2 shows the performance of various PVA membranes in dehydrating of IPA [51–55]. As observed, incorporation of the MWNTs to the PVA matrix enhances the performance of the prepared nanocomposite membranes. As shown, permeation flux of the prepared membrane is higher compared with that of most nanocomposite membranes and also selectivity of the prepared nanocomposite membranes increases with addition of the MWNT-PAH.

4. Conclusion

MWNTs were prepared via the CVD method. The as-grown MWNTs were characterized using FESEM and HR-TEM. PAH was used for wrapping the MWNTs for better dispersion in the PVA

matrix. The PAH-wrapped MWNTs showed good dispersion in the PVA solution. FESEM observation confirmed that the MWNT-PAH interacts with the PVA matrix well. Incorporation of the MWNT-PAH into the PVA matrix improved the performance of the prepared nanocomposite membranes in PV separation. But, at the higher content of MWNT-PAH, selectivity decreases due to the agglomeration of MWNT-PAH. Also, addition of the MWNT-PAH into the PVA casting solution reduced DS of the prepared nanocomposite membranes.

Acknowledgment

The authors gratefully acknowledge the financial support of this project by New Technology Research Group, Petrochemical Research and Technology Co. of Iran (Grant no. 0870289002).

Nomenclature

J	Permeation flux [kg/m ² h]
W	Mass of permeate [kg]
A	Effective membrane area [m ²]
t	Time [s]
P_w	Mass percent of water in permeate [%]
P_{IPA}	Mass percent of IPA in permeate [%]
F_w	Mass percent of water in feed [%]
F_{IPA}	Mass percent of IPA in feed [%]
PSI	Pervaporation separation index
DS	Degree of swelling [%]
W_s	Weights of swollen membrane [kg]
W_d	Weights of dry membrane [kg]
S_a	Mean roughness
S_q	Root mean square of the Z data
S_z	Mean difference between the highest peaks and the lowest alleys [nm]

Greek letters

α_{sep}	Separation selectivity
----------------	------------------------

References

- [1] S. Zereskhi, A. Figoli, S.S. Madaeni, S. Simone, M. Esmailinezhad, E. Drioli, Effect of polymer composition in PEEKWC/PVP blends on pervaporation separation of ethanol/cyclohexane mixture, *Separation and Purification Technology* 75 (2010) 257–265.
- [2] M. Mulder, *Basic Principles of Membrane Technology*, second edition ed., Kluwer Academic Publishers, Netherlands, 1998.
- [3] B. Smitha, D. Suhanya, S. Sridhar, M. Ramakrishna, Separation of organic-organic mixtures by pervaporation: a review, *Journal of Membrane Science* 241 (2004) 1–21.
- [4] R.Y.M. Huang, *Pervaporation Membrane Separation Processes*, Elsevier Science Publishers, Amsterdam, Netherlands, 1991.
- [5] S. Xiao, R.Y.M. Huang, X. Feng, Preparation and properties of trimesoyl chloride crosslinked poly(vinyl alcohol) membranes for pervaporation dehydration of isopropanol, *Journal of Membrane Science* 286 (2006) 245–254.
- [6] Y. Zhu, S. Xia, G. Liu, W. Jin, Preparation of ceramic-supported poly(vinyl alcohol)-chitosan composite membranes and their applications in pervaporation dehydration of organic/water mixtures, *Journal of Membrane Science* 349 (2010) 341–348.
- [7] H. Cong, M. Radosz, B.F. Towler, Y. Shen, Polymer-inorganic nanocomposite membranes for gas separation, *Separation and Purification Technology* 55 (2007) 281–291.
- [8] T.S. Chung, L.Y. Jiang, Y. Li, S. Kulprathipanja, Mixed matrix membranes (MMMs) comprising organic polymers with dispersed inorganic fillers for gas separation, *Progress in Polymer Science* 32 (2007) 483–507.

- [9] Z. Huang, Y. Shi, R. Wen, Y. Guo, J. Su, T. Matsuura, Multilayer poly(vinyl alcohol)-zeolite 4A composite membranes for ethanol dehydration by means of pervaporation, *Separation and Purification Technology* 51 (2006) 126–136.
- [10] Y.L. Liu, C.Y. Hsu, Y.H. Su, J.Y. Lai, Chitosan-silica complex membranes from sulfonic acid functionalized silica nanoparticles for pervaporation dehydration of ethanol-water solutions, *Biomacromolecules* 6 (2005) 368–373.
- [11] De Q. Vu, W.J. Koros, S.J. Miller, Mixed matrix membranes using carbon molecular sieves: I. Preparation and experimental results, *Journal of Membrane Science* 211 (2003) 311–334.
- [12] A.F. Ismail, P.S. Goh, S.M. Sanip, M. Aziz, Transport and separation properties of carbon nanotube-mixed matrix membrane, *Separation and Purification Technology* 70 (2009) 12–26.
- [13] X.L. Xie, Y.W. Mai, X.P. Zhou, Dispersion and alignment of carbon nanotubes in polymer matrix: a review, *Materials Science and Engineering* 49 (2005) 89–112.
- [14] Y.T. Ong, A.L. Ahmad, S.H.S. Zein, K. Sudesh, S.H. Tan, Poly(3-hydroxybutyrate)-functionalised multi-walled carbon nanotubes/chitosan green nanocomposite membranes and their application in pervaporation, *Separation and Purification Technology* 76 (2011) 419–427.
- [15] L. Qu, Y. Lin, D.E. Hill, B. Zhou, W. Wang, X. Sun, A. Kitaygorodskiy, M. Suarez, J.W. Connell, L.F. Allard, Y.-P. Sun, Polyimide-functionalized carbon nanotubes: synthesis and dispersion in nanocomposite films, *Macromolecules* 37 (2004) 6055–6060.
- [16] M.J. O'Connell, P. Boul, L.M. Ericson, C. Huffman, Y. Wang, E. Haroz, C. Kuper, R.E. Smalley, Reversible water-solubilization of single-walled carbon nanotubes by polymer wrapping, *Chemical Physics Letters* 342 (2001) 265–271.
- [17] E.E. Hill, Y. Lin, A.M. Rao, L.F. Allard, Y.-P. Sun, Functionalization of carbon nanotubes with polystyrene, *Macromolecules* 35 (2002) 9466–9471.
- [18] S.E. Baker, W. Cai, T.L. Lasseter, K.P. Weidkamp, R.J. Hamers, Covalently bonded adducts of deoxyribonucleic acid (DNA) oligonucleotides with single-wall carbon nanotubes: synthesis and hybridization, *Nano Letters* 2 (2002) 1413–1417.
- [19] A. Eitan, K. Jiang, D. Dukes, R. Andrews, L.S. Schadler, Surface modification of multiwalled carbon nanotubes: toward the tailoring of the interface in polymer composites, *Chemistry of Materials* 15 (2003) 3198–3201.
- [20] S. Banerjee, T. Hemraj-Benny, S.S. Wong, Covalent surface chemistry of single-walled carbon nanotubes, *Advanced Materials* 17 (2005) 17–29.
- [21] K. Balasubramanian, M. Burghard, Chemically functionalized carbon nanotubes, *Small* 1 (2005) 180–192.
- [22] M.A. Aroon, A.F. Ismail, M.M. Montazer-Rahmati, T. Matsuura, Effect of chitosan as a functionalization agent on the performance and separation properties of polyimide/multi-walled carbon nanotubes mixed matrix flat sheet membranes, *Journal of Membrane Science* 364 (2010) 309–317.
- [23] Z.Q. Zhang, B. Liu, Y.L. Chen, H. Jiang, K.C. Hwang, Y. Huang, Mechanical properties of functionalized carbon nanotubes, *Nanotechnology* 19 (2008) 395702.
- [24] C.-Y. Hong, Y.Z. You, C.-Y. Pan, New approach to functionalize multi-walled carbon nanotubes by the use of functional polymers, *Polymer* 47 (2006) 4300–4309.
- [25] P. Bertrand, A. Jonas, A. Laschewsky, R. Legras, Ultrathin polymer coatings by complexation of polyelectrolytes at interfaces: suitable materials, structure and properties, *Macromolecular Rapid Communications* 7 (2000) 319–348.
- [26] P. Hammond, Recent explorations in electrostatic multilayer thin film assembly, *Current Opinion in Colloid and Interface Science* 6 (1999) 430–442.
- [27] C. Iamsamai, A. Soottitantawat, U. Ruktanonchai, S. Hannongbua, S.T. Dubas, Simple method for the layer-by-layer surface modification of multiwall carbon nanotubes, *Carbon* 49 (2011) 2039–2045.
- [28] H. Kong, P. Luo, C. Gao, D. Yan, Polyelectrolyte-functionalized multiwalled carbon nanotubes: preparation, characterization and layer-by-layer self-assembly, *Polymer* 46 (2005) 2472–2485.
- [29] F. Peng, Z. Jiang, C. Hu, Y. Wang, L. Lu, H. Wu, Pervaporation of benzene/cyclohexane mixtures through poly(vinyl alcohol) membranes with and without [beta]-cyclodextrin, *Desalination* 193 (2006) 182–192.
- [30] A.M. Sajjan, B.K. Jeevan Kumar, A.A. Kittur, M.Y. Kariduraganavar, Novel approach for the development of pervaporation membranes using sodium alginate and chitosan-wrapped multiwalled carbon nanotubes for the dehydration of isopropanol, *Journal of Membrane Science* 425–426 (2013) 77–88.
- [31] G.M. Spinks, S.R. Shin, G.G. Wallace, P.G. Whitten, S.I. Kim, S.J. Kim, Mechanical properties of chitosan/CNT microfibrils obtained with improved dispersion, *Sensors and Actuators B: Chemical* 115 (2006) 678–684.
- [32] M. Olek, M. Hilgendorff, Michael Giersig, A simple route for the attachment of colloidal nanocrystals to noncovalently modified multiwalled carbon nanotubes, *Colloids and Surfaces A: Physicochemical and Engineering Aspects* 292 (2007) 83–85.
- [33] S.H.H.C.L. Li, D.J. Liaw, K.R. Lee, J.Y. Lai, Interfacial polymerized thin-film composite membranes for pervaporation separation of aqueous isopropanol solution, *Separation and Purification Technology* 62 (2008) 696.
- [34] W.L.L.S.H. Huang, D.J. Liaw, C.L. Li, S.T. Kao, D.M. Wang, K.R. Lee, J.Y. Lai, Characterization, transport and sorption properties of poly(thiol ester amide) thin-film composite pervaporation membranes, *Journal of Membrane Science* 322 (2008) 139.
- [35] S. Mosso, G. Fanchini, A. Tagliaferro, Growth of vertically aligned carbon nanotubes by CVDs by evaporation of carbon precursors, *Diamond and Related Materials* 14 (2005) 784.
- [36] S. Porro, S. Musso, M. Gioecelli, Study of CNTs and nanographite grown by thermal CVD using different precursors, *Journal of Non-Crystalline Solids* 352 (2006) 1310.
- [37] M. Kumar, Y. Ando, A simple method of producing aligned carbon nanotubes from an unconventional precursor – comphor, *Chemical Physics Letters* 374 (2003) 521.
- [38] B.C. Satishkumar, A. Govindaraj, C.N.R. Rao, Bundles of aligned carbon nanotubes obtained by the pyrolysis of ferrocene-hydrocarbon mixtures: role of the metal nanoparticles produced in situ, *Chemical Physics Letters* 307 (1999) 158–162.
- [39] R. Andrews, D. Jacques, A.M. Rao, F. Derbyshire, D. Qian, X. Fan, E.C. Dickey, J. Chen, Continuous production of aligned carbon nanotubes: a step closer to commercial realization, *Chemical Physics Letters* 303 (1999) 467–474.
- [40] Y. Shirazi, M.A. Tofighy, T. Mohammadi, A. Pak, Effects of different carbon precursors on synthesis of multiwall carbon nanotubes: purification and functionalization, *Applied Surface Science* 257 (2011) 7359–7367.
- [41] A.A. Khodadadi, M. Maghrebi, Y. Mortazavi, A. Sane, Y. Shirazi, M. Rahimi, Z. Tsakadze, S. Mhaisalkar, Effect of acetic acid on amorphous carbon removal along a CNT synthesis reactor, *Journal of Optoelectronics and Advanced Materials* 11 (2009) 1611–1617.
- [42] E. Nativ-Roth, R. Shvartzman-Cohen, C. Bounioux, M. Florent, D. Zhang, I. Szeleifer, R. Yerushalmi-Rozen, Physical adsorption of block copolymers to SWNT and MWNT: a nonwrapping mechanism, *Macromolecules* 40 (2007) 3676.
- [43] M. Olek, T. Busgen, Michael Hilgendorff, Michael Giersig, Quantum dot modified multiwall carbon nanotubes, *Journal of Physical Chemistry B* 110 (2006) 12901–12904.
- [44] J.-H. Choi, J. Jegal, W.-N. Kim, Fabrication and characterization of multi-walled carbon nanotubes/polymer blend membranes, *Journal of Membrane Science* 284 (2006) 406–415.
- [45] S. Qiu, L. Wu, X. Pan, L. Zhang, H. Chen, C. Gao, Preparation and properties of functionalized carbon nanotube/PSF blend ultrafiltration membranes, *Journal of Membrane Science* 342 (2009) 165.
- [46] Y. Shirazi, M.A. Tofighy, T. Mohammadi, Synthesis and characterization of carbon nanotubes/poly vinyl alcohol nanocomposite membranes for dehydration of isopropanol, *Journal of Membrane Science* 378 (2011) 551.
- [47] M. Naebe, T. Lin, W. Tian, L. Dai, X. Wang, Effects of MWNT nanofillers on structures and properties of PVA electrospun nanofibres, *Nanotechnology* 18 (2007) 225605.
- [48] O. Probst, E.M. Moore, D.E. Resasco, B.P. Grady, Nucleation of polyvinyl alcohol crystallization by single-walled carbon nanotubes, *Polymer* 45 (2004) 4437–4443.
- [49] R.S. Karupppannan, J.G. Varghese, M.Y. Kariduraganavar, Development of hybrid membranes using chitosan and silica precursors for pervaporation separation of water isopropanol mixtures, *Journal of Chemical and Engineering Data* 55 (2010) 2084–2092.
- [50] Y.C. Liu, J.W. Shen, K.E. Gubbins, J.D. Moore, T. Wu, Q. Wang, Diffusion dynamics of water controlled by topology of potential energy surface inside carbon nanotubes, *Physical Review B – Condensed Matter and Materials Physics* 77 (2008) 125438.
- [51] S. Razavi, A. Sabetghadam, Dehydration of isopropanol by PVA-APTEOS/TEOS nanocomposite membranes, *Chemical Engineering Research and Design* 89 (2011) 148–155.
- [52] Q.G. Zhang, Q.L. Liu, Y. Chen, J.H. Chen, Dehydration of isopropanol by novel poly(vinyl alcohol)-silicone hybrid membranes, *Industrial and Engineering Chemistry Research* 46 (2007) 913–920.
- [53] M. Sairam, B.V.K. Naidu, S.K. Nataraj, B. Sreedhar, T.M. Aminabhavi, Poly(vinyl alcohol)-iron oxide nanocomposite membranes for pervaporation dehydration of isopropanol 1,4-dioxane and tetrahydrofuran, *Journal of Membrane Science* 283 (2006) 65–73.
- [54] S.G. Adoor, B. Prathab, L.S. Manjeshwar, T.M. Aminabhavi, Mixed matrix membranes of sodium alginate and poly(vinyl alcohol) for pervaporation dehydration of isopropanol at different temperatures, *Polymer* 48 (2007) 5417–5430.
- [55] Z. Gao, Y. Yue, W. Li, Application of zeolite-filled pervaporation membrane, *Zeolites* 16 (1996) 70–74.